2026 IEEE/SICE International Symposium on System Integration (SII)
January 11-14, 2026. Cancún, México

Modeling and Evaluation of Soft Gears for Wearable Robots*

Takeshi Kido[1], Keisuke Osawa[2], Kiyotaka Ikejo[3], Akio Ueda[4],
D.S.V Bandara[2], Jumpei Arata[2], Eiichiro Tanaka[5]

Abstract— **With global aging, the incidence of motor dysfunction is increasing. Especially, the upper limb motor dysfunction requires assistance and rehabilitation to involve in daily activities such as eating and brushing one's teeth. In recent decades, wearable robots have made remarkable progress, with a wide variety of upper limb assistive robots being developed and commercialized. However, it relies on a control system using sensors and software, and there is a possibility that a sudden collision could damage the wearable robots or the users. Therefore, to further improve safety, it is desirable to add mechanical safety devices such as torque limiters. In previous studies, we proposed a new torque limiter with a soft gear transmission mechanism and verified its feasibility. On the other hand, to apply this torque limiter to wearable robots, it is necessary to model the deformation behavior of the soft gear and establish a design methodology. In this study, we proposed a modeling method for soft gears and conducted the evaluation experiments using a finite element analysis and a prototype. The proposed model predicted slip torque values of 0.78 Nm (forward) and 1.54 Nm (reverse), with an error rate of approximately 13% from the experimental values. Wearable robots equipped with the soft gears have the potential to improve safety and be used in daily life.**

I. INTRODUCTION

With the global aging of the population, the incidence of motor function impairments is increasing. In particular, the risk of stroke increases significantly with age, and it has been reported that more than 70% of stroke patients are aged 65 or older[1]. Against this background, there is a growing demand for wearable assistive devices that support functional recovery and daily living activities after stroke. In recent years, the development of wearable assistive devices has rapidly advanced. For the upper limbs, exoskeleton-type products such as HAL Single Joint and MyoPro have already been commercialized, and their effectiveness has been reported [2][3]. A number of systems have been proposed that integrate real-time control using multiple sensors, such as inertial measurement units (IMUs), surface electromyography (sEMG), and encoders [4]. These systems can estimate the user's motion intent based on sensor data and provide highly accurate assistance. However, these systems rely on software-based control. As a result, unexpected collisions or external forces can still cause mechanical damage to internal components. Actually, there have been reported cases where servo motor gears were damaged due to unexpected overloads, even though the control system was functioning properly, highlighting the importance of mechanical safety devices [5][6].

Mechanical safety mechanisms include variable stiffness actuators (VSAs) [7], series elastic actuators (SEAs) [8], and torque limiters. VSAs enhance safety by dynamically changing joint stiffness based on the applied torque. However, they tend to be structurally complex and bulky. SEAs improve force control accuracy by inserting elastic elements between the motor and the joint. However, they do not necessarily prevent overloads caused by sudden impact. Torque limiters can physically disconnect power transmission when torque exceeds a threshold. Their simple structure and high responsiveness make them particularly suitable for applications where protection from external force is essential. For these reasons, this study focuses on torque limiters. Conventional torque limiters, such as ball-detent type, friction type, and magnetic type, are widely used in many engineering applications. However, these mechanisms are usually implemented in a separate space for the torque limiter, which not only increases the number of parts and points of failure, but also requires installation space along the shaft axis. In small robots and wearable assistive devices where space and weight are severely restricted, these additional mechanisms can significantly reduce design flexibility and hinder miniaturization. To overcome these limitations, we proposed a new torque limiter using "soft gears" that integrate the torque limiting function into the gear transmission in previous study [9]. Soft gears are made of flexible material, and when excessive load is applied, the teeth elastically deform and slip, preventing torque transmission. This approach enables overload protection to be implemented without the additional components. In this study, we propose a modeling method to predict the slip torque of soft gears. By assuming the soft gear teeth as cantilevers, slip torque can be estimated using a simple method based on the theory of material mechanics. This will simplify the design of soft gear and enable its implementation in wearable robots. The validity

*This work was supported by JSPS KAKENHI Grant Number JP23K17236 and Frontiers in Engineering Research from Kyushu University (FY2025-2026)

[1]T. Kido is with the Faculty of Systems Life Sciences, Kyushu University, Fukuoka 8190395, Japan. (email: kido.takeshi.108@s.kyushu-u.ac.jp)

[2]K. Osawa, D.S.V. Bandara, J. Arata are with the Department of Mechanical Engineering, Faculty of Engineering, Kyushu University, Fukuoka 8190395, Japan. (email: k-osawa@mech.kyushu-u.ac.jp; d-sanjaya@mech.kyushu-u.ac.jp; jumpei@mech.kyushu-u.ac.jp)

[3]K. Ikejo is with the Graduate School of Advanced Science and Engineering, Hiroshima University, Higashi-hiroshima 7398527, Japan. (email: ikejo@hiroshima-u.ac.jp)

[4]A. Ueda is with the Amtec Inc., Osaka 5520007, Japan. (email: ueda@amtecinc.co.jp)

[5]E. Tanaka is with the Graduate School of Information, Production and Systems, Waseda University, Kitakyushu 808135, Japan. (email: tanakae@waseda.jp)

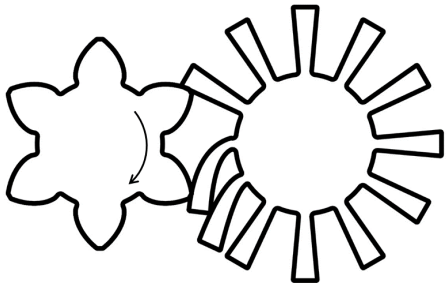

(a) Elastic deformation and slippage of soft gear teeth under forward-input

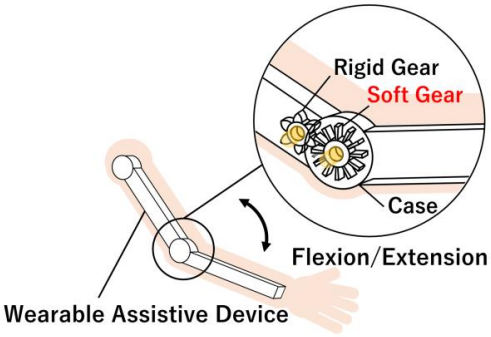

(b) Application image in a wearable assistive device

Fig. 1. Concept of proposed torque limiter using soft gear

of the proposed model was verified through comparison with experimental results using a finite element analysis (FEA) and a prototype. In this paper, we report the concept of torque limiter, modeling methodology, prototype fabrication using a 3D printer, and evaluation results.

II. METHOD

A. Concept

Soft gears are made of flexible materials and are designed to hinder torque transmission by elastically deforming and slipping the teeth under overload conditions. In this study, we adopted an inconvertibility cycloid tooth profile proposed by Narimatsu et al. [10], which achieves a high reduction ratio. This tooth profile consists of a combination of epicycloid and hypocycloid curve (Fig. 1). When the rolling circle radius of the hypocycloid is set to half the reference circle radius, the calculated tooth profile is geometrically straight. In previous study [9], it was shown that this straight tooth profile allows for smooth meshing even when there is a slight deviation in the center distance. This is also because soft gears are made of flexible materials and the teeth deform elastically. This approach allows the integration of a torque limiter into the power transmission mechanism, contributing to the miniaturization and weight reduction of the entire system. In addition, by adjusting the center distance, the slip torque can be changed.

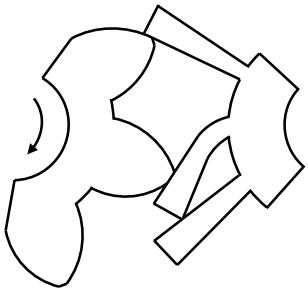

(a) Deformation behavior when forward-input

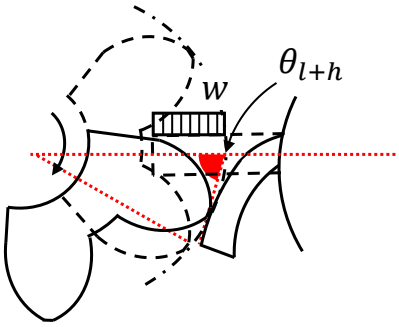

(b) Geometric condition at the onset of slip

Fig. 2. Schematic diagram of soft gear tooth deformation and slippage under forward-input

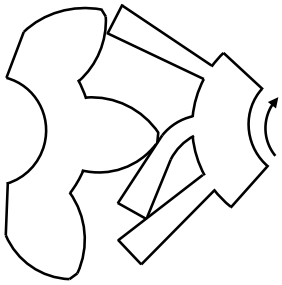

(a) Deformation behavior when reverse-input

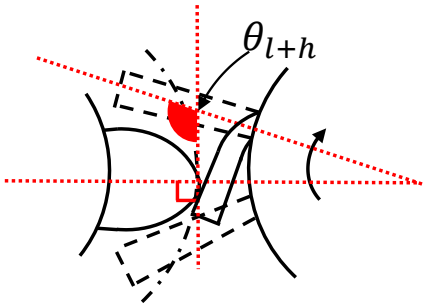

(b) Geometric condition at the onset of slip

Fig. 3. Schematic diagram of soft gear tooth deformation and slippage under reverse-input

B. Theoretical Model

In this study, a theoretical model was constructed to predict the slip torque by approximating the soft gear tooth as a cantilever beam.

- **Forward-input slip torque**: When the rigid gear stops, the soft gear does not slip. When the rigid gear rotates, it causes slippage in the soft gear, preventing torque transmission (Fig. 2(a)). For example, during operation, unexpected external forces such as stumbling or collision may apply reverse torque, causing the teeth to slip and protect the system from damage.
- **Reverse-input slip torque**: The rigid gear is fixed, and the soft gear slips and rotates (Fig. 3(a)). The soft gear allows the user to apply external force to move the arm voluntarily.

In both cases, the slip torque is calculated based on the elastic deformation of the soft gear and static equilibrium. The force acting on single tooth is derived, and the contact ratio is considered to determine the total slip torque. Here, the contact ratio ε of the inconvertibility cycloid gear can be expressed as follows [10].

$$\varepsilon = \frac{a}{\pi m} \cos^{-1} \left\{ 1 - \frac{r_t'^2 - r'^2}{2a(r' + a)} \right\} \tag{1}$$

Where a is the rolling circle radius, m is the module, r is the reference circle radius, and r_t is the root circle radius. Variables without a prime (') refer to the soft gear (hypocycloid gear), while variables with a prime refer to the rigid gear (epicycloid gear). In the proposed theoretical model, the effects of friction and large deformation are ignored for simplicity, and it cannot accommodate changes in slip torque due to changes in center distance.

1) Forward-input slip torque: Let the length of the meshing region be l and the length of the non-meshing region be h, and assume that a distributed load w acts on the meshing region. Under these conditions, the deflection angle θ_{l+h} can be expressed as follows.

$$\theta_{l+h} = \frac{wlh}{2EI}(l + h) + \frac{wl^3}{6EI} \tag{2}$$

Where E is the Young's modules, and I is the moment of inertia of area. Assuming the gear tooth as a cantilever beam with a uniform rectangular cross-section, the moment of inertia of area I can be expressed as follows.

$$I = \frac{bt^3}{12} \tag{3}$$

Where b is the face width, t is the tooth tip thickness. As shown in Fig. 2(b), when slippage occurs, the tooth tip of the soft gear aligns with the tooth tip of the rigid gear. Therefore, the deflection angle θ_{l+h} can be expressed as follows.

$$\theta_{l+h} = \frac{\pi}{2} - \frac{\pi}{2z'} \tag{4}$$

Where z is the number of teeth. From Eq.(2) and Eq.(3), the distributed load w can be derived as follows.

$$w = \frac{6EI}{\{3lh(l + h) + l^3\}} \left(\frac{\pi}{2} - \frac{\pi}{2z'} \right) \tag{5}$$

Assuming the same distributed load w acts on the rigid gear, the forward-input slip torque T_f can be calculated as follows.

$$\begin{aligned} T_f &= wl \left(r_t' - \frac{l}{2} \right) \varepsilon \\ &= \frac{6EIl\varepsilon}{3lh(l + h) + l^3} \left(\frac{\pi}{2} - \frac{\pi}{2z'} \right) \left(r_t' - \frac{l}{2} \right) \end{aligned} \tag{6}$$

2) Reverse-input slip torque: With reverse input, the rigid gear is fixed, and the soft gear rotates (Fig. 3(a)). In this case, it is assumed that a distributed load w also occurs. Then, the deflection angle θ_{l+h} can be expressed as follows.

$$\theta_{l+h} = \frac{wlh}{2EI}(l + h) + \frac{wl^3}{6EI} \tag{7}$$

When slippage occurs, the rotation angle of the soft gear corresponds to the angular pitch, as shown in Fig. 3(b). Based on this behavior, the deflection angle θ_{l+h}, the distributed load w, and the reverse-input slip torque T_r can be described as follows.

$$\theta_{l+h} = \frac{\pi}{2} + \frac{\pi}{z} \tag{8}$$

$$w = \frac{6EI}{\{3lh(l + h) + l^3\}} \left(\frac{\pi}{2} + \frac{\pi}{z} \right) \tag{9}$$

$$\begin{aligned} T_r &= wl \left(r_t - \frac{l}{2} \right) \varepsilon \\ &= \frac{6EIl\varepsilon}{3lh(l + h) + l^3} \left(\frac{\pi}{2} + \frac{\pi}{z} \right) \left(r_t - \frac{l}{2} \right) \end{aligned} \tag{10}$$

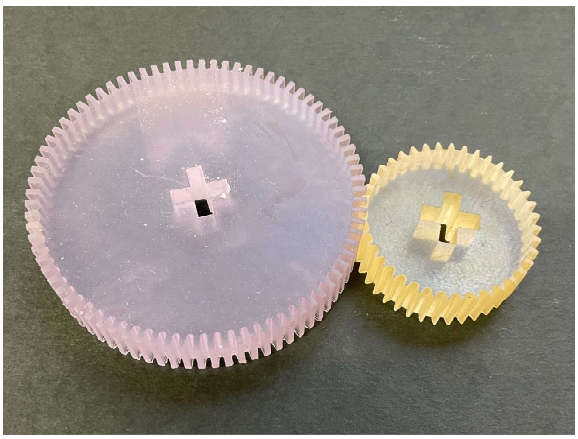

Fig. 4. A sample image of the prototype using a 3D printer

TABLE I

GEAR SPECIFICATIONS OF SOFT AND RIGID GEARS

Parameter	Unit	Hypocycloid (Soft gear)	Epicycloid (Rigid gear)
Type	–	Hypocycloid (Soft gear)	Epicycloid (Rigid gear)
Module	mm	1	1
Number of teeth	–	80	40
Reference circle radius	mm	40	20
Rolling circle radius	mm	20	20
Root circle radius	mm	36.6	19.8
Face width	mm	15	15
Material	–	Flexible80A (Rubber)	AR-M2 (Acrylic)
Young's modulus	MPa	9.6	3000
Poisson's ratio	–	0.49	0.35

C. Design

The design specifications of the proposed soft gear are shown in TABLE I. In wearable robots, the size and weight of the components directly affect user's comfort, wearability, and range of motion. Therefore, the gear dimensions must be carefully selected to avoid excessive physical burden on the user. Based on an anthropometric database, the average forearm circumference of elderly males can be calculated to be approximately 80 mm [11]. Thus, the tip diameter of the gear must be set to less than that to ensure wearability. Therefore, the tip diameter of the soft gear was set to 80 mm. In addition, the face width of 15 mm and a module of 1.0 mm were selected as the design that would provide sufficient strength and allow slipping, considering stress values.

D. Fabrication

We used a stereolithography 3D printer (Form3B+, Formlabs Inc., USA) to fabricate a prototype of the soft gear. High-precision additive manufacturing is possible with a layer pitch of 50 µm. The material used is a rubber-like resin (Flexible 80A, Formlabs Inc., USA). In addition, to fabricate a prototype of the rigid gear, we used an inkjet-based 3D printer (AGILISTA-3200, Keyence Co., Japan). This printer also allows for high-precision additive manufacturing, with a layer pitch of 15 µm. The material is a transparent acrylic resin (AR-M2, Keyence Co., Japan). A sample image of the prototype using a 3D printer is shown in Fig. 4.

III. EVALUATION

A. FEA

To calculate the slip torque, a static structural analysis was performed using Ansys Workbench R2 2023 (Ansys Inc., USA). For the forward-input slip torque, the axis of the soft gear (large, hypocycloid gear) was fixed to the ground, and the axis of rigid gear (small, epicycloid gear) was set as a rotational joint, and rotated until the soft gear tooth slipped completely. For the reverse-input slip torque, the axis of the rigid gear was fixed to the ground, and the axis of soft gear was set as a rotational joint, and rotate until the soft gear tooth slipped completely. The maximum torque values under these analysis conditions were calculated as the slip torque. To investigate the effect of center distance on slip torque, the analysis was repeated by varying the center distance from 60.0 mm (the theoretical center distance which the gears mesh ideally) to 61.0 mm in 0.10 mm increments. A frictional contact (coefficient of friction: 0.05) was defined between the contact surfaces of the two gears. The materials used for each gear and their mechanical properties are listed in TABLE I.

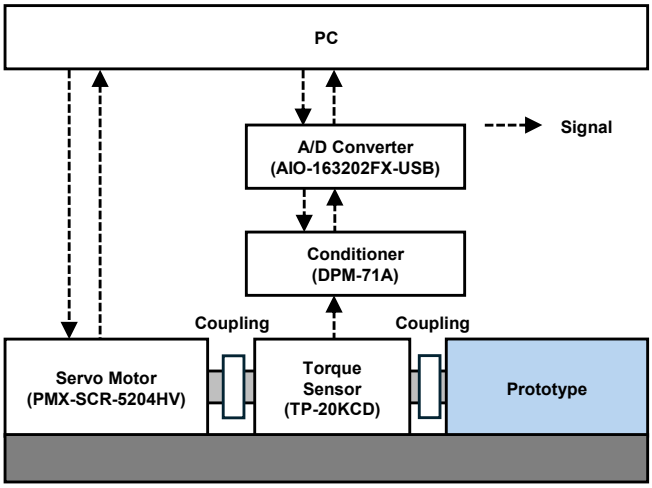

(a) Block diagram of the measurement system

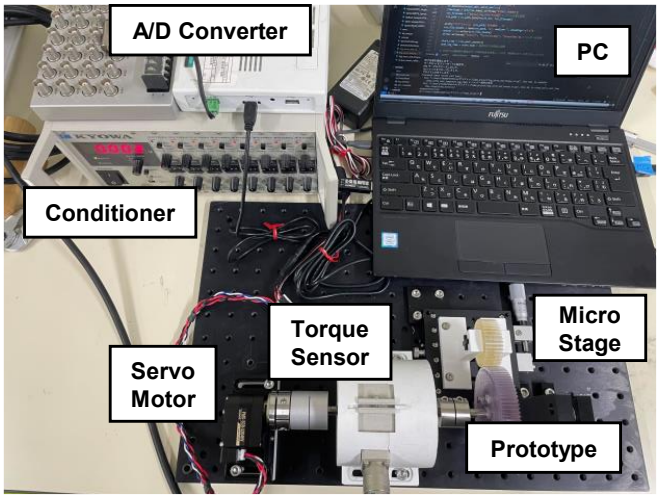

(b) Overview of the experimental setup

Fig. 5. Experimental setup for slip torque measurement

TABLE II
COMPARISON OF SLIP TORQUE VALUES

Input type	Experiment [Nm]	FEA [Nm]	Theoretical [Nm]
Forward	0.699	0.674	0.781
Reverse	1.34	1.30	1.54

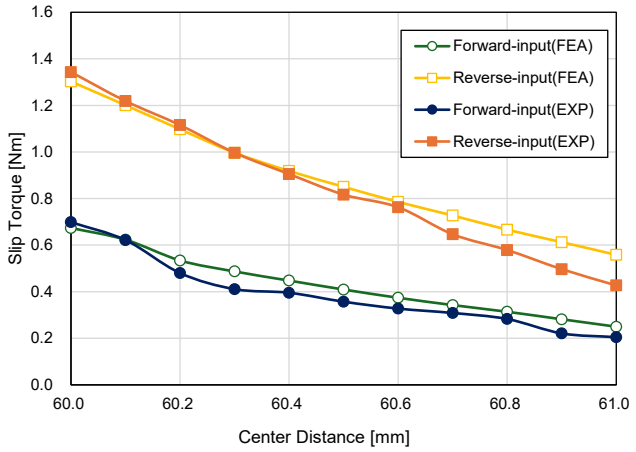

Fig. 6. Relationship between center distance and slip torque

B. Experiment

To measure the experimental values of slip torque and evaluate the validity of the proposed theoretical model, an experimental test was conducted using a torque sensor.

1) Forward-input slip torque: Fig. 5(a) shows a block diagram of the measurement system, and Fig. 5(b) shows a schematic diagram of the experimental setup. In the experiment, the rigid gear was mounted on the shaft of a torque sensor, while the soft gear was fixed to prevent rotation. The rigid gear was rotated by a servo motor installed on the opposite side of the torque sensor, causing it to engage and slip against the fixed soft gear. During the test, torque and angular displacement were recorded. All equipment was controlled via a PC, and the data was logged on the PC. The experiment was repeated three times for each condition, and the average of the peak torque values was defined as the forward-input slip torque. The center distance was varied from the theoretical meshing distance of 60.0 mm to 61.0 mm in 0.10 mm increments.

2) Reverse-input slip torque: The experimental setup was the same as for the forward-input slip torque. However, to measure the reverse-input slip torque, the soft gear was mounted on the shaft of a torque sensor, while the rigid gear was fixed. The experiment was repeated three times for each condition, and the average of the peak torque values was defined as the reverse-input slip torque. The center distance was varied from the theoretical meshing distance of 60.0 mm to 61.0 mm in 0.10 mm increments.

C. Result

In this study, the relationship between slip torque and center distance was evaluated through three approaches:

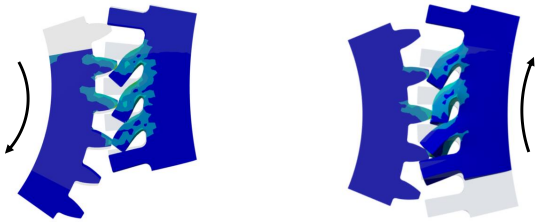

(a) Under forward-input (b) Under reverse-input

Fig. 7. FEA results showing tooth deformation and slip behavior

experimental measurement (EXP), finite element analysis (FEA), and theoretical calculation (TH). Fig. 6 illustrates how the slip torque varied with center distance under both forward-input and reverse-input conditions. A comparison of the slip torque values obtained at a nominal center distance of 60.0 mm is summarized in TABLE II. In both input directions, slip torque showed a gradual decreasing trend as the center distance increased from 60.0 mm to 61.0 mm. This behavior can be attributed to the shallower meshing of gear teeth at larger center distances, which reduces the reaction force and facilitates earlier onset of slippage.

Under reverse-input conditions, the slip torque decreased approximately 1.35 Nm at 60.0 mm to 0.40 Nm at 61.0 mm (70% reduction). For forward-input conditions, the slip torque gradually decreased from 0.70 Nm to 0.20 Nm over the same range (71% reduction). These results clearly demonstrate the sensitivity of slip torque to center distance variation. When comparing the results from the three methods, it was observed that the difference between the FEA and experimental values became more pronounced as the center distance increased. This discrepancy is likely due to differences in boundary conditions, contact behavior, and material modeling. Despite these quantitative differences, FEA exhibited consistent qualitative trends, affirming that the FEA simulations effectively captured the slip characteristics of the soft gear system. The theoretical model was applied only at the nominal center distance of 60.0 mm and did not evaluate variations in center distance. At this condition, the predicted slip torque was 0.78 Nm for forward input and 1.54 Nm for reverse input (Error rate: 13.0%), which closely matched the experimental results of 0.70 Nm and 1.34 Nm (Error rate: 10.3%). Although the theoretical model has some limitations, its predictive accuracy at the nominal center distance supports its validity as a simplified analytical tool. Overall, all three approaches (EXP, FEA, and TH) produced results with consistent trends. These findings confirm that the slip torque of the soft gear system can be adjusted by changing the center distance, providing a tunable mechanical safety feature.

IV. DISCUSSION

The theoretical model proposed in this study approximates the soft gear tooth as a cantilever beam subjected to a distributed load. This simplified equation provides a framework for estimating slip torque under static conditions. At the center distance of 60.0 mm, the theoretical values aligned

well with both FEA and experimental values, indicating that the proposed model is effectiveness for rapid estimation of slip behavior in the nominal configuration. However, the model omits several key factors that significantly affect the actual behavior:

- Changes in geometric conditions such as center distance
- Friction between meshing gears
- Effect of large deformation
- Nonlinear material characteristics such as viscoelasticity and hyper-elasticity

Ignoring these factors is primary reason for the observed discrepancies between the theoretical and experimental results.

The proposed model does not consider the geometric deformation that occurs as the center distance changes, limiting its applicability beyond the design condition. In both FEA and experiments, slip torque consistently decreased as the center distance increased. This trend is attributed to reduced contact meshing between the gear teeth, which reduces the elastic restoring force and results in earlier slip. Although the simplified theoretical model cannot capture this behavior, it was clearly confirmed in both FEA and experiments. Nonetheless, slight differences were observed among the three methods. As the center distance increased, the deviation between FEA and experimental results became more pronounced. This may stem from multiple factors. First, idealized boundary conditions and material parameters were used in the FEA simulations, which do not perfectly reflect the actual experimental conditions. Second, mechanical play, assembly errors, and shaft misalignment may have affected the experimental results. Third, the soft material used for the gear, Flexible 80A, exhibits viscoelastic and velocity-dependent behavior that is difficult to accurately capture using static theoretical models or linear elastic FEA. Future challenge should consider nonlinear dynamic models that incorporating time-dependent material behavior.

On the other hand, the slip torque can be adjusted by changing the center distance, which has practical advantages in applications to rehabilitation device. During early stages of rehabilitation, a lower torque threshold can be set to prevent excessive stress on the joint, while in later stages, the reduction of center distance can increase torque transmission for enhanced support. This adjustability allows the torque limiter to be tailored to the patient's recovery stage, providing a safer and more adaptable assistive mechanism.

V. Conclusion

In this study, we proposed a modeling methodology of soft gears for wearable robots and demonstrated its validity using FEA and a prototype. By modeling the soft gear teeth as a cantilever beam, a simplified theoretical framework was established to estimate the slip torque during overload. The evaluation results showed consistent trends across the theoretical calculations at the nominal center distance (Error rate : Within approximately 13%). This confirmed that the proposed model can reasonably approximate slip behavior under static conditions, despite certain simplifications such as ignoring friction, large deformations, and material nonlinearity. In addition, the slip torque can be tuned by adjusting the center distance between gears. This feature provides a practical advantage for applications such as wearable assistive devices, where torque thresholds may need to be customized according to the rehabilitation phase or user condition. The main contribution of this paper is to present a modeling method for soft gears and demonstrate their applicability to wearable robots. This represents important step toward the development of a practical wearable robots equipped with a torque limiter.

Future works include developing a more accurate prediction model that considers changes in center distance, nonlinear deformation, viscoelasticity, and dynamic behavior. Furthermore, we will evaluate durability and vibration response characteristics under repeated loading, optimize materials, and design an overall system, aiming for practical applications such as rehabilitation robots.

References

[1] M. Kelly-Hayes. "Influence of age and health behaviors on stroke risk: Lessons from longitudinal studies", Journal of the American Geriatrics Society, vol. 58, no. S2, pp. S325-328, 2010.

[2] E. W. Tan, S. C. Chai, Y. Sankai, M. Shingu, N. A. Razaob, and H. Hussain. "Single Joint Hybrid Assistive Limb (HAL-SJ) robotic exoskeleton therapy in improving functional outcomes among workers with wrist fractures: Study protocol for a randomized controlled trial", PLoS One, vol. 20, no. 4, e0322191, 2025.

[3] S. Pundik, J. McCabe, M. Skelly, A. Salameh, J. Naft, Z. Chen, C. Tatsuoka, and S. Fatone. "Myoelectric Arm Orthosis in Motor Learning-Based Therapy for Chronic Deficits After Stroke and Traumatic Brain Injury", Frontiers in Neurology, vol. 13, 791144, 2022.

[4] A. Kapsalyamov, S. Hussain, and P.K. Jamwal. "State-of-the-Art Assistive Powered Upper Limb Exoskeletons for Elderly", IEEE Access, vol. 8, pp. 178991-179001, 2020.

[5] J. R. Zhuang, H. Nagayoshi, H. Kondo, K. Muramatsu, K. Watanuki, and E. Tanaka. "Development of a torque limiter for the gear of an assistive walking device", Journal of Advanced Mechanical Design, Systems, and Manufacturing, vol. 11, no. 6, 17-00376, 2017.

[6] K. Osawa, Y. Hua, K. Duan, K. Nakagawa, and E. Tanaka. "Development of a Compact Walking Assistive Robot for Exercise Promotion and Gait Training", Emerging Technologies and Future Work, vol.117, pp. 98-106, 2023.

[7] B. Vanderborght, A. Albu-Schaeffer, A. Bicchi, E. Burdet, D. G. Caldwell, R. Carloni, M Catalano, O. Eiberger, W. Friedl, G. Ganesh, M. Grebenstein, G. Grioli, S. Haddadin, H. Hoppner, A. Jafari, M. Laffaranchi, D. Lefeber, F. Petit, S. Stramigioli, N. Tsagarakis, M. V. Damme, R. V. Ham, L. C. Visser, and S. Wolf. "Variable impedance actuators: A review, Robotics and Autonomous Systems", vol. 61, iss. 12, pp. 1601-1614, 2013.

[8] C. Lee, S. Kwak, J. Kwak, and S. Oh. "Generalization of Series Elastic Actuator Configurations and Dynamic Behavior Comparison", Actuators, vol. 6, no. 3, 26, 2017.

[9] T. Kido, K. Osawa, K. Ikejo, A. Ueda, D.S.V. Bandara, J. Arata, and E. Tanaka. "Design and analysis of soft gear for application to torque limiter", Proceedings of the 10th International Conference on Manufacturing, Machine Design and Tribology (ICMDT2025), pp. 266-267, 2025.

[10] N. Narimatsu, K. Ikejo, and D. Irikado. "Design and performance of small tooth number gears using cycloid curves", Proceedings of the Japan Society for Design Engineering Chugoku Branch Conference, pp. 33-38, 2022. (in Japanese)

[11] Digital Human Research Team, Artificial Intelligence Research Center, AIST, "Digital Human Body Dimensions Database (1991-92): F26. Forearm circumference", available at: https://www.airc.aist.go.jp/dhrt/91-92/data/search6.html, accessed Aug. 27, 2025.